Desalination and Water Treatment
www.deswater.com

13 (2010) 74–81
January

1944-3994/1944-3986
doi: 10.5004/dwt.2010.1052

Water hammer simulation in spiral wound reverse osmosis membranes

S. A. Avlonitis*, D.A. Avlonitis, A. Baldoukas, K. Kralis, A. Metaxa

Laboratory of Quality Control, Operations Management and Process Engineering, Technological Institute (T.E.I.) of Chalkidas, 34400 Psaxna EVIA, Greece
Tel. +3022280 99650; Fax +3022280 99649; email: savlon@teihal.gr

Received 2 April 2009; accepted 25 November 2009

ABSTRACT

The purpose of this work is the development of a mathematical model for the formation and the propagation velocity of water hammer in spiral wound reverse osmosis (RO) membranes. Unexpected shutdowns of the RO plants and failure of the check valves can cause water hammer formation and its propagation as a pressure wave inside the membrane envelope resulting in membrane destruction.

The model is based on energy and mass balances at flow conditions inside the membrane envelope. The mathematical analysis results in explicit equations for the local permeate pressure in steady state conditions and the increase of pressure in unsteady situations. During the water hammer formation the permeate pressure may increase so as to cause damaging results to the RO membranes.

Keywords: Destruction of RO membranes; Water hammer; Flow in porous media

1. Introduction

Water hammer is a phenomenon that is caused by the sudden decrease of the water flow. This may be the result of manipulating a valve in pipes, or a sudden RO plant shut down. It may also arise in a RO system. The result of the water hammer formation is an increase in pressure, which is transmitted along the fluid approximately at the local speed of sound of in the fluid in the piping system. The maximum pressure developed by the phenomenon of water hammer depends on the rate of water flow, the structure of the piping, the materials of the piping, and so forth (Williams [1] and Kawaguchi et al. [2]). This maximum is, in cases, about ten times as high as that of the pressure of the water at steady conditions. If the water hammer occurs repeatedly it may cause fatigue of the material. Water hammer may occur not only during valve operation but also in connection with any abnormal flow conditions, such as pump failure.

An historical review of the development of the theory of water hammer was presented by A. Bergant et al. [3]. Joukowsky [4] has derived the law for instantaneous water hammer for the piezometric head rise resulting from a fast closure of a downstream valve based on his experimental findings. The modelling of the water hammer phenomena can be accomplished simply by Joukowsky's equation or by other computational techniques of flow dynamics, such as finite element method (FEM) or the method of characteristics (MOC) [5,6]. Many researchers have used hybrid models, with the method of characteristics (MOC) modelling the water hammer equations and the finite element method (FEM) modelling the structure [7]. In carrying out water hammer calculations, it is important to use the accurate value for the speed of propagation

*Corresponding author

Presented at the conference on Desalination for the Environment: Clean Water and Energy, 17–20 May 2009, Baden-Baden, Germany. Organized by the European Desalination Society.

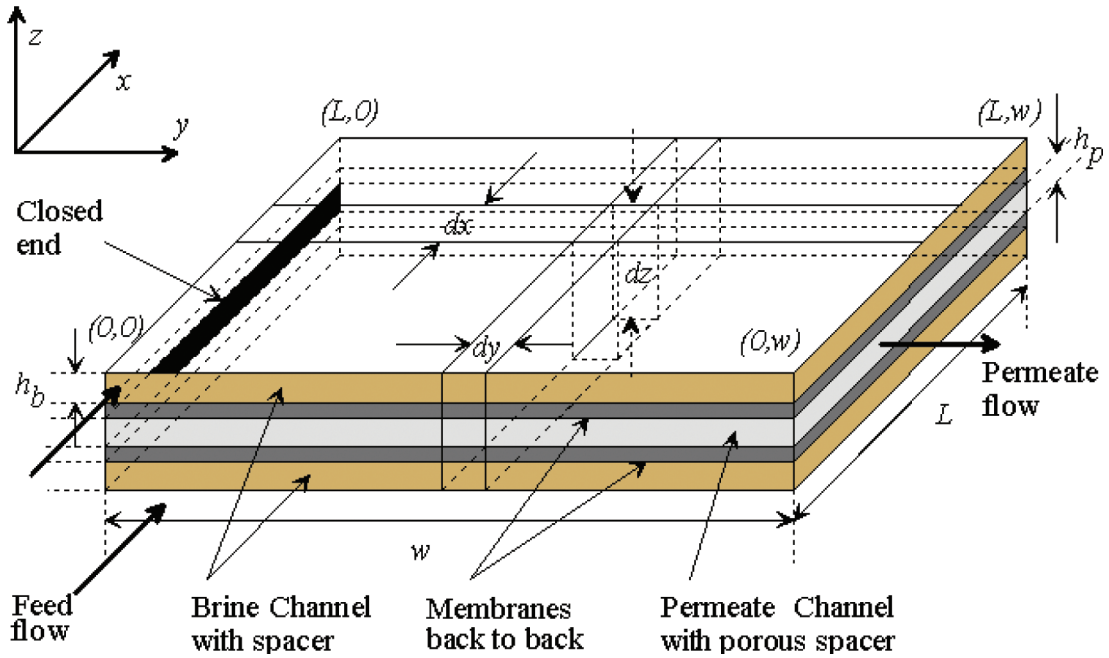

Fig. 1. Unwound spiral wound RO membrane module.

of the resulting pressure waves. It is known that because of the expansion of the piping system the speed of the pressure wave propagation is less than that of the sonic velocity in the liquid. An experimental study to estimate this velocity in the case of a plexiglas pipe was presented by H.H. Safwat [8]. The material of the piping system is an important factor in the case of water hammer formation. Different polymeric materials fiber-reinforced or not have been tested towards the water hammer effects [2,8,9].

The purpose of this work is to develop an explicit equation for the pressure in the permeate channel and apply this equation to the water hammer formation. This semi-analytical approach can simulate the water hammer formation insight the RO membrane envelope. The developed equation can be useful to determine the maximum permeate pressure that the membrane undertakes even under unsteady conditions.

2. Theory

The flow of the water in the permeate channel in RO spiral wound membrane modules can be reduced to the flow in a rectangular porous channel with elastic walls from aromatic polyamides, see Fig. 1.

The two membranes are kept apart by a porous media placed in the permeate channel. The permeate water travels from the closed end along the permeate channel to the open end, (0,*w*) and (*L*,*w*). A full picture of the membranes, spacers and the collecting tube at the open end of each membrane envelope is presented in Fig. 2. The two membranes back to back and the permeate spacer, which are glued in the three sides, form the membrane envelope. The open end of the envelope is connected with the collecting tube.

A complete list of the assumptions, which this work is based on for the derivation of the permeate water velocity and pressure at steady state conditions, is given in Table 1.

A detailed presentation of the mathematical model has been presented elsewhere [10,11] The flow conditions in these flat channels are changing at every point (*x*,*y*). The basic working equation for the permeate water flux at every local point (*x*,*y*), based on solution diffusion theory is equation,

$$J(x,y) = k_1 \Delta P_{ef}(x,y) \tag{1}$$

where $J(x,y)$ is the local water flux, k_1 is the water permeability coefficient and $\Delta P_{ef}(x,y)$ is the local effective pressure.

A simple mass and momentum balance in the permeate channel gives the equations,

$$\frac{\partial u_p(x,y)}{\partial y} = \frac{2J(x,y)}{h_p} \tag{2}$$

$$\frac{\partial P_p(x,y)}{\partial y} = -k_{fp}\mu u_p(x,y) \tag{3}$$

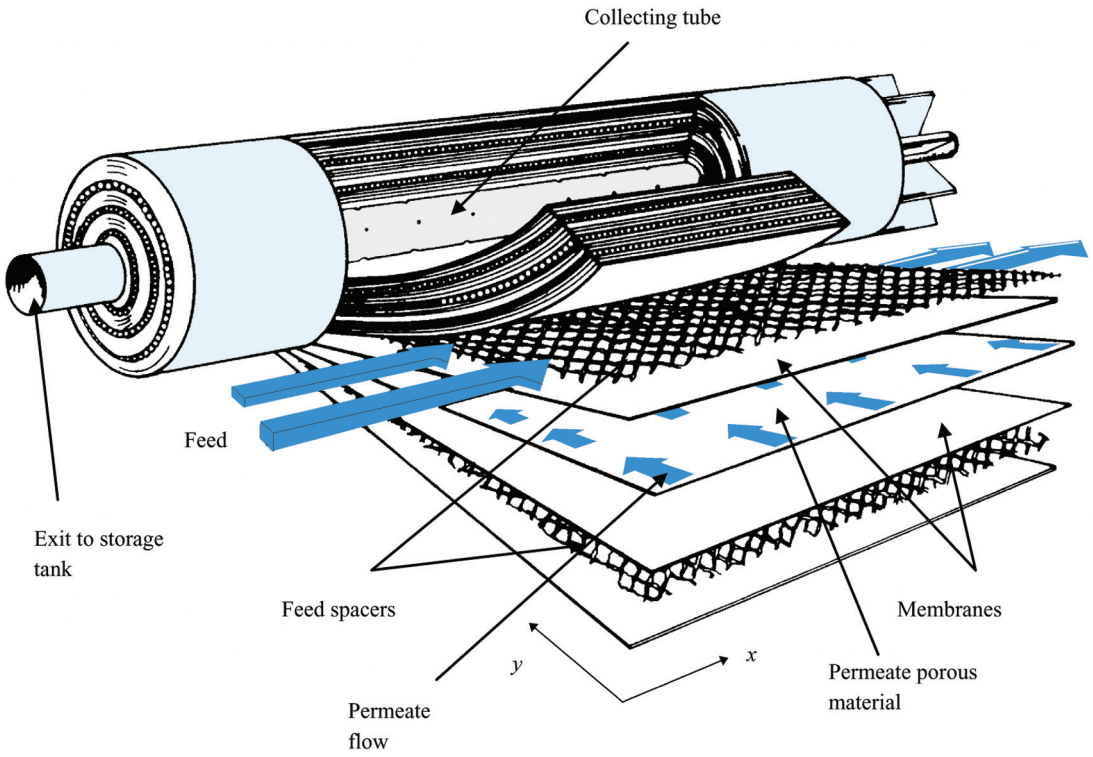

Fig. 2. General layout of RO-ED-WAIV process. Spiral wound RO membrane module.

where, $u_p(x,y)$ is the local permeate velocity, h_p is the permeate channel height, μ is the viscosity of the feed solution, y is the distance in the y axis and k_{fp} is the friction coefficient in the permeate channel.

A combination of Eqs. (1) and (2) taking into account the relation for $\Delta P_{ef}(x,y)$, results in the following Equation [11].

Table 1
Assumptions for the 2-dimension flow calculations

1. Validity of Darcy's law for permeate and brine channel.
2. Validity of solution-diffusion model, for the transport of water through the membrane. No flow restrictions for the locally produced permeate in the porous substructure of the composite membrane.
3. Immediate and complete mixing of the locally produced permeate water with the bulk flow in the permeate channel.
4. The permeate concentration has been neglected in comparison to the feed concentration.
5. Membrane modules are made up of flat channels, with constant geometrical shape, see Fig. 1
6. Constant fluid properties.
7. Negligible components of brine and permeate velocities along the y (tangential) and x (axial) axis respectively.
8. Negligible diffusive mass transport along the x and y direction in both channels. This means that the flux through the membrane due to diffusion is much smaller to the flux due to convection. The driving force for the water transport is the effective pressure across the membrane.
9. The brine concentration varies linearly with the distance L, in the axial direction. $c_b(x) = c_f + fx$ (A.1)
   where, $f = \frac{c_b(L)-c_f}{L}$ (A.2)
   The value of f is an indication of the recovery ratio R.
10. Validity of the thin film theory, with the approximation which is given by Eq. (A.3). $c_{bw} = c_b\left(1+\frac{J}{k}\right)$ (A.3)
11. A constant mass transfer coefficient, given by Eq. (A.4) $\mathrm{Sh} = 0.63 \times Sc^{0.17} \times \mathrm{Re}_f^{0.40} \times \left[\frac{c_f}{\rho}\right]^{-0.77} \times \left[\frac{P_f}{P_o}\right]^{-0.55}$ (A.4)
12. Osmotic pressure proportional to the concentration, see Eq. (A.5). $\pi = \omega \times c$ (A.5)

$$u_p(x,y) = \frac{2qk_1k\sinh\frac{y}{q}}{h_p\left[k + k_1\omega\left(c_f + fx\right)\right]\cosh\frac{w}{q}} \left[\Delta P - \omega c_f + \frac{c_f u_f k_{fb}\mu}{f}\ \ln\frac{c_f}{c_f + fx} - \omega fx\right] \quad (4)$$

Where, k is the mass transfer coefficient, c_f is the feed concentration, ΔP is the pressure difference given by $(P_f(0,w) - P_p(0,w))$, w is the width of the membrane, k_{fp} is the friction coefficient in the permeate channel and $q = \sqrt{\frac{h_p}{2k_1k_{fp}\mu}}$.

The permeate pressure can be assumed constant in the x direction so that an integration of Darcy's law Eq. (3), taking into account the permeate velocity profile, Eq. (4), will result in the final Eq. (5). This equation gives the permeate pressure at any point in the y direction insight the membrane envelope at steady state flow conditions. The pressure, in the x direction is assumed constant, since there is no flow in the x direction in the permeate side.

$$P_p(y) = \frac{2k_{fp}\mu k k_1 q^2}{h_p[k + k_1\omega c_f]} \times \left[\Delta P - \omega c_f\right] \times \left[1 - \frac{\cos\ h\frac{y}{q}}{\cos\ h\frac{w}{q}}\right] + P_p(0,w) \quad (5)$$

where $P_p(y)$ is the local permeate pressure and $P_p(0,w)$ is 10^5 Pa.

In the previous analysis the flow is steady because both permeate velocity and pressure does not change with the time. However, if unexpected electricity shut down occurs in an RO plant or an emergency situation requires an immediate shut down, then the flow conditions are becoming unsteady and permeate pressure and velocity can vary with time. In most RO plants the permeate water travels through the permeate pipe to the storage tank that is always at higher level than the RO membrane modules. As a result, the abnormal stop of the operation of a RO plant is equivalent to the sudden decrease of the flow of a liquid in a rectangular closed conduit that is caused by the manipulation of a valve. This is actually the formation of a water hammer. Although in real situation there is always a check valve to prevent the water hammer propagation towards the membranes, the possibility of a check valve failure can not be disregarded.

The theoretical examination of this phenomenon can be accomplished if a valve is fitted at the exit of the permeate tube of a RO module. Suppose the valve is closed instantaneously or very fast that is $T_c << 2w/V$, where V the velocity of the pressure wave, w the width of the permeate channel, T_c the valve closure time and $u_p(x,y)$ the velocity at each local point. This results to a complete interruption of the flow of the liquid near the valve. Far away of the valve, inside the membrane envelope the water is still moving with velocity $u_p(x,y)$ at each local point, so that near the valve the water is compressed, increasing its pressure and density. The pressure wave, which is formed, travels along the permeate channel towards the closed end of the permeate envelope with a rapid velocity ($V >> u_p(x,y)$). The increase in pressure, Δp, due to the water hammer, and the velocity of propagation of pressure wave, V, are the two unknown quantities that can be determined by Eqs. (6) and (7) [4,9,12].

$$\Delta p = \rho V u_p(x,y), \quad (6)$$

where ρ is the density of the water,

$$V = \sqrt{\frac{\frac{K}{\rho}}{1 + \frac{K}{E}\times\frac{d}{e}}} \quad (7)$$

where K is the bulk module of the fluid, E is the Young's modules of the pipe wall material, d *is* the inner diameter of the pipe and e is the wall thickness. Eq. (6) expresses an one dimensional flow, in y direction. There is no flow in the x direction, The symbol $u_p(x,y)$ shows the local value of the velocity at any (x,y) point. Eq. (7) can be approximated for pipes with rigid walls to Eq. (8) [13], which is the Newton's equation for speed of sound through any elastic medium.

$$V = \sqrt{\frac{K}{\rho}} \quad (8)$$

Taking the value of K for the water at 25 °C as 2.2×10^9 N/m^2 and $\rho = 997$ kg/m^3[14], the value of V is found to be 1,485 m/s for pipes with rigid walls.

For pipe with elastic walls, as well as for RO membranes, Eq. (7) should be used. The Young's module value of aromatic polyamide membranes, which are the walls of the permeate channel, was considered to be $E = 2,54 \times 10^9$ N/m^2 [15]. For non-circular closed conduits, it is necessary to replace the diameter d in Eq. (7) by the hydraulic diameter, d_h, see Eq. (9), taking into account the rectangular shape of the permeate channel [12].

$$d_h = \frac{4A}{\Pi} \quad (9)$$

where A is the cross-sectional area and Π is the wetted perimeter of the conduit.

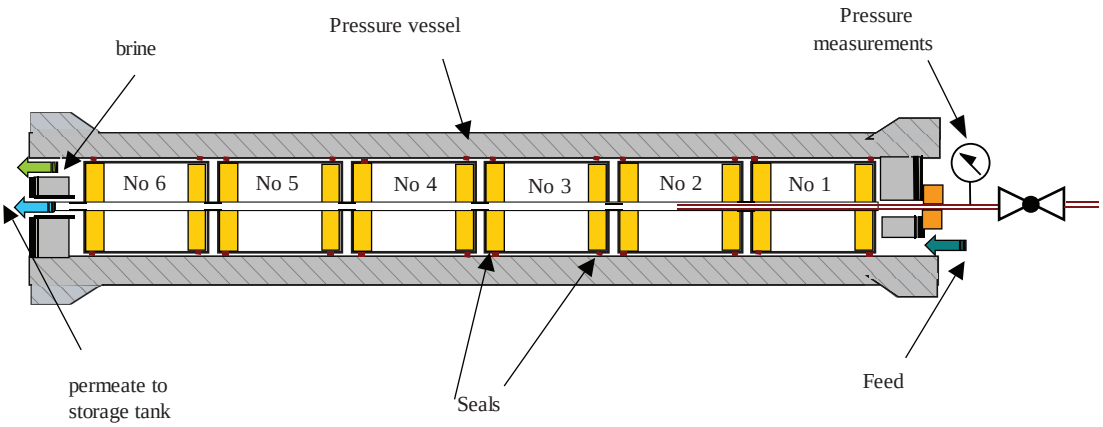

Fig. 3. Experimental set up for permeate water pressure.

A combination of Eqs. (4), (6) and (7) gives the following final equation, of the increase in pressure in the permeate channel of the RO membranes due to the water hammer formation:

$$\Delta p(x,y) = \rho\sqrt{\frac{\frac{K}{\rho}}{1+\frac{K}{E}\times\frac{d_h}{e}}}\times\frac{2qk_1k\sin\ h\frac{v}{q}}{h_p\left[k+k_1\omega\left(c_f+fx\right)\right]\cos\ h\frac{w}{q}} \times\left[\Delta P-\omega c_f+\frac{c_f u_f k_{fb}\mu}{f}\ln\frac{c_f}{c_f+fx}-\omega fx\right] \tag{10}$$

It should be pointed out that the velocity is not constant at any point in the permeate channel even at steady flow conditions. Therefore, the increase in pressure due to water hammer formation is not expected to be constant in the permeate channel. As it was mentioned before the flow is only in the y direction.

3. Experimental membrane data

In real industrial RO plants the pressure vessels contain in most cases six (6) membrane modules in a row, see Fig. 3. Experimental data were collected from an industrial plant with a capacity of 380 m^3/day, based in Santorini island (Greece). The plant includes six (6) pressure vessels, each one containing six (6) membrane modules. The membranes were SW30HR-380 made by FilmTec. The feed seawater had a concentration of 42.000 ppm and the temperature was 25 °C.

The measurements of the permeate pressure in the collecting tube of each membrane do not show significant variation as a function of the membrane position. Pressure measurements at various positions were taken by inserting a hypodermic tube of suitable length. The maximum pressure $P_p(0,w)$ at the exit of the membrane was 1.85 bar at module No 1 and the minimum pressure was 1.80 bar at module No 6, see Table 2. This permeate pressure is a function of the permeate flow rate, which is related to the applied pressure, the feed concentration and the recovery ratio. As it was expected the maximum permeate rate is in membrane No 1 due to the lower feed concentration and the maximum applied pressure.

4. Results and discussion

The theoretical permeate pressure variation insight the membranes envelopes at steady conditions, according to Eq. (5), is presented in Fig. 4.

Table 2
Permeate pressure in collecting tubes as a function of the membrane module number

Run-1. $Q_{p,\ total} = 15.77\ m^3/h$, $Q_{f,\ total} = 43.77\ m^3/h$, $\Delta P = 62$ bar, $c_{p,\ total} = 586$ ppm						
Membrane No	No1	No2	No3	No4	No5	No6
P_p at exit (bar)	1.85	1.85	1.85	1.80	1.80	1.80
Run-2. $Q_{p,\ total} = 13.68\ m^3/h$, $Q_{f,\ total} = 43.77\ m^3/h$, $\Delta P = 57$ bar, $c_{p,\ total} = 630$ ppm						
Membrane No	No1	No2	No3	No4	No5	No6
P_p at exit (bar)	1.60	1.60	1.60	1.55	1.55	1.55

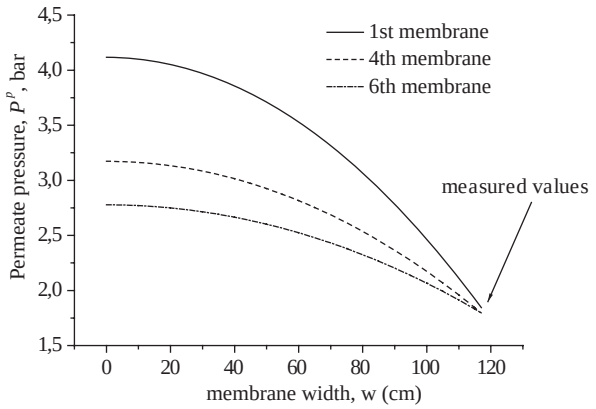

Fig. 4. Permeate pressure profiles for the different membrane modules at 25 °C, $c_f = 42$ kgr/m^3, $Q_f = 45$ m^3/h and $\Delta P = 62$ bar.

It is illustrated very clearly that the local permeate pressure decreases from the first membrane module to the last one. It can be concluded therefore that the maximum permeate pressure is at the first membrane at the point (0,0). The No1 membrane has the highest permeate flow due to the lowest feed concentration. As a result of that it would be expected that if a hydraulic hammer occurs during operation, the first membrane module is more likely to be damaged in the glue strips of the membrane envelop.

For SW30HR-380 RO membranes made by FilmTec with dimensions $L = 0.866$ m, $h_m = 0.14 \times 10^{-3}$m and $h_p = 0.52 \times 10^{-3}$m, the hydraulic diameter is calculated by the use of Eq. (9) as $d_h = 1.039 \times 10^{-3}$m. Application of Eq. (7) for the previous data gives $V = 545$m/s for the velocity of the of propagation of pressure wave in the permeate channel of the SW30HR-380 RO membranes.

At the operating conditions presented in Fig. 3 the permeate flow rate of the six membrane modules is $Q_p = 7.268 \times 10^{-4}$ m^3/s. This is the maximum flow rate at the exit of the sth membrane module. Taking into account the diameter of the collecting tube ($d_t = 0.029$ m) the maximum permeate velocity at the exit is $u_{max} = 1.101$ m/s. If the water hammer formation takes place at the end of the collecting tube, exit of the 6th membrane module, which is more likely, then the application of Eq. (6) at the exit yields a maximum increase in pressure at $\Delta p = 5.9 \times 10^5$ Pa. This increase in pressure will travel inside the collecting tube, will insert into the membrane envelopes from the exit of the permeate channel towards the closed end and might damage the membranes. It must be stated that at the closed end of the membrane envelope the operating permeate pressure at steady state conditions is over 4.0×10^5 Pa. Similar values have been found experimentally [10]. According the mathematical model and the calculations presented in this work the time for a round trip of a pressure wave, starting at the exit of the pressure envelope, is $t_t = 2w/V = 4.29 \times 10^{-3}$ s.

Although the water hammer is more likely to be formed at the exit of the collecting tube of the pressure vessels of the membranes, Eq. (10) may serve to predict also the water hammer formation inside the permeate channel of the membrane envelopes. It is unlikely that a water hammer occurs inside the permeate channel. However, it can not be excluded, for example when glue strips have blocked the permeate flow or the permeate envelop has a closed end in the collecting tube due to manufacturing defects or when debris accumulation exists.

Eq. (10) was applied for the first and the sixth membrane modules, since these are the two extreme cases. The dimensions and the characteristic constants of this type of membranes are presented in appendix A. The estimation of the feed, brine and permeate characteristics for the first and sixth membrane module can be accomplished by the use of ROSA 6.1 software [16]. The operating conditions and the results of these calculations are presented in Table 3.

The results of the application of Eq. (10) for SW30HR-380 membranes for the initial values of the water hammer formation at any point of the permeate channel, with realistic data from an industrial plant as presented in Table 3, are illustrated in Fig. 5 for the No 1 membrane module.

As long as the water hammer is formed it travels along the permeate channel towards the closed end of the membrane envelope. It is seen from Fig. 5 that the initial formation of water hammer insight the membrane is not really a problem. This is due to the low

Table 3
Operating conditions and calculated variables for membrane No 1 and No 6 at 25 °C

	Experimental data		Calculated variables				
	c_f (kg/m^3)	$P(0,w)$ (bar)	c_b (kg/m^3)	Q_f (m^3/s)	Q_p (m^3/s)	u_f (m/s)	f (kg/m^4)
Membrane No1	42.000	61,66	46.194	2.055×10^{-3}	1.86×10^{-4}	0.14	4.84
Membrane No6	61.105	63.760	60.70	1.41×10^{-3}	6.11×10^{-5}	0.096	3.06

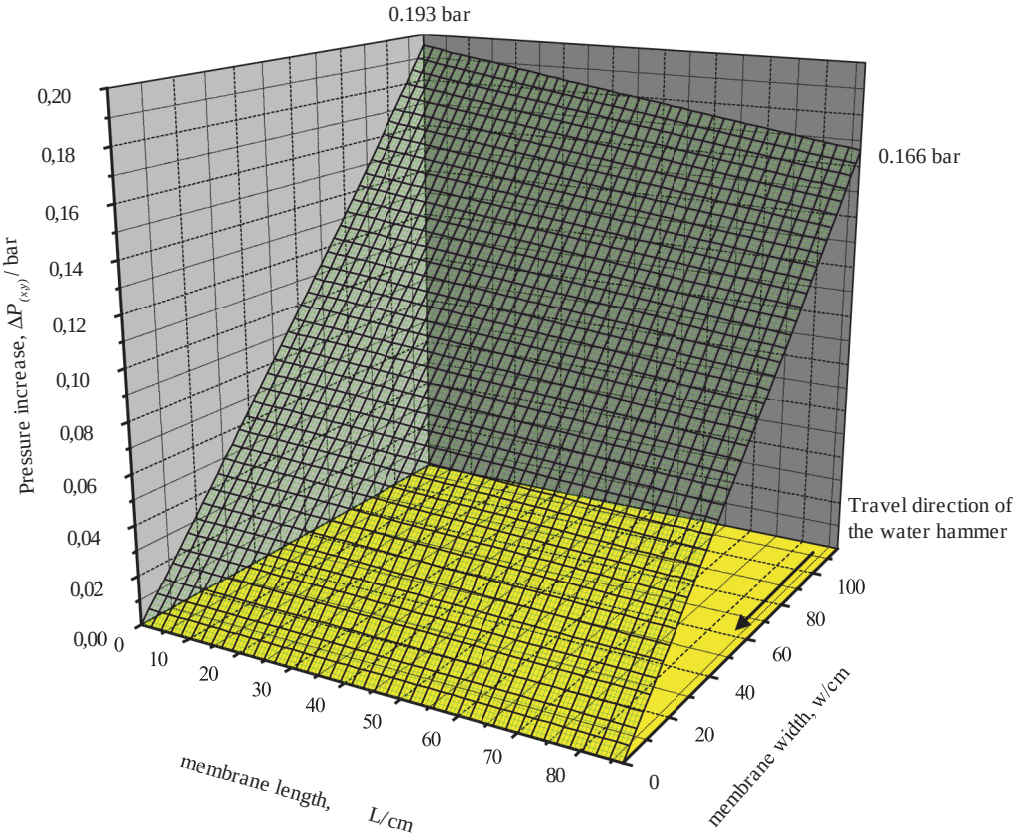

Fig. 5. The local water hammer formation in the permeate channel of No 1 membrane.

permeate velocity. A similar graph can be found for the 6th membrane, although the maximum increase in pressure (0.085×10^5 Pa) is less than for the first membrane due to much less permeate flow rate.

5. Conclusion

A simple and a straight forward procedure to determine the water hammer formation and the increase in pressure was presented in this work. It was found that if water hammer conditions are created in the collecting tube, then the increase in pressure in the permeate channel can rise up to six (6) bar. This increase in pressure will travel along the permeate channel giving a total pressure more than ten (10) bar that might result in the destruction of the membrane. This may be an explanation of various cases where membrane destruction have been observed after reated unexpected shutdowns of the plant.

On the other hand if a water hammer occurs inside the permeate channel the increase in pressure can be neglected.

Appendix A

Dimensions of the 8'' SW30HR380 modules and the values of the constants for the membrane performance.

Permeate channel height (mm)	$h_p = 0.52$
Brine channel height (mm)	$h_b = 0.84$
Membrane height (mm)	$h_m = 0.14$
Total membrane length (cm)	$L_2 = 96.50$
Active membrane length (cm)	$L = 86.65$
Total membrane width (cm)	$w_2 = 134$
Active membrane width (cm)	$w = 117$
Active membrane area (m^2)	$A = 35.00$
Water permeability coefficient cm s^{-1} bar^{-1}	$k_1 = 4.2 \times 10^{-5}$
Mass transfer coefficient (cm/s)	$k = 2.7 \times 10^{-3}$
Permeate friction parameter (cm^{-2})	$k_{fp} = 1,100,000$
Permeate friction parameter (cm^{-2})	$k_{fb} = 309 \times \mathrm{Re}_f^{0.83}$
Osmotic pressure coefficient (bar cm^3 gr^{-1})	$\omega = 728$
Number of leaves in 8'' SW30HR380	$N = 13$

Symbols

A	cross sectional area, m^2
c	concentration, kg $^{-1}$
d	inner diameter, m
dh	hydraulic diameter, m
e	wall thickness, m
E	Young's module, N m^{-2}
f	constant defined by Eq. (A.2), kg m^{-4}
ΔP_{ef}	driving Pressure, Pa
ΔP	pressure difference given by (P_f(0,w) − P_p(0,w)), Pa
Δp	Pressure increase due to water hammer, Pa
h	height, m
J	average volumetric flux, m s^{-1}
K	Bulk module, N m^{-1}
k	mass transfer coefficient, m s^{-1}
k_1	water permeability coefficient, m s^{-1} bar^{-1}
k_f	friction parameter, m^{-2}
L	membrane length (axial), m
$L2$	membrane length with glue, m
P	pressure, Pa
Pf	applied pressure at the inlet of the pressure vessel, Pa
P°	constant (10^5)
q	constant for a given membrane and temperature, defined by $q = \sqrt{\frac{h_p}{2k_1 k_{fp}\mu}}$, m
Q	Flow rate, m^3/s
Re	Reynolds number ($\mathrm{Re} = hu\rho/\mu$)
Sc	Schmidt number ($\mathrm{Sc} = \mu/\rho D$)
Sh	Sherwood number ($\mathrm{Sh} = kh_b/D$)
T	Temperature, K
u	velocity, m/s
V	velocity of propagation of water hammer, m/s
w	membrane width (tangential), m
w_2	membrane width with glue, m
x	coordinate along the membrane length, m
y	coordinate along the membrane width, m

Greek letters

μ	viscosity, kg m^{-1} s^{-1}
Π	perimeter, m
π	osmotic pressure, Pa
ρ	density, kg/m^3
ω	osmotic pressure coefficient, N m kg^{-1}

Subscript

b	brine
ef	effective
f	feed
m	membrane
p	permeate

References

[1] D.J. Williams, Water hammer in non-rigid pipes. Precursor waves and mechanical damping, J. Mech. Eng. Sci., 19 (1997) 237.

[2] T. Kawaguchi, H. Nishimura, K. Ito, T. Kuriyama and I. Narisawa, Resistance of glass fiber-reinforced thermoplastics to water hammer, Polymer Testing, 22 (2003) 327-333.

[3] A. Bergant, A.R. Simpson and A.S. Tijsseling, Water hammer with column separation: a historical review, J. Fluid. Struct., 2(2) (2006) 135-171.

[4] N. Joukowsky, On the hydraulic hammer in water supply pipes, Mémoires de L' Académie Impériale des Sciences de St.-Pétersbourg, Series 8, vol. 9, No. 5 (in German).

[5] A.S. Tijisseling, Fluid-structure interaction in liquid-filled systems: a review, J. Fluid. Struct., 10 (1996) 109-146.

[6] D.C. Wiggert, F.J. Hatfield and S. Struckenbruck, Analysis of liquid and structural transients in piping by the method of characteristics, ASME J. Fluid. Eng. 109 (1987) 161-165.

[7] A.G.T.J. Heinsbroek, Fluid-structure interactions in non-rigid pipeline systems, Nucl. Eng. Des., 172 (1997) 123-135.

[8] J.D. Rawles, J.A. Roscow and M.G. Phillips, The effect of transient overloads on the long term performance of glass fiber reinforced polymer (GFRP) pipes for power station cooling water system, Am. Soc. Mech. Eng. Pres. Ves. Pip. Div., 196 (1990) 17.

[9] M.H. Ho, J.R. Hwang and J.L. Doong, Impact fatigue of a polycarbonate/acrylonitrile-butadiene-styrene blend, Polymer Eng. Sci., 39 (1999) 708.

[10] S.A. Avlonitis, et al., Spiral wound modules performance. An analytical solution: Part II, Desalination, 89 (1993) 227-246.

[11] S. Avlonitis and D. Papanikas, Flow parameters profiles in cross-flow of a two component fluid through semipermeable membranes, Separ. Sci. Technol., 32(5) 1997 939-950.

[12] D.N. Roy, Applied Fluid Mechanics, East-West Press, 1st ed., New Delhi, India, 1987.

[13] B.S. Masssey, Mechanics of Fluids, Chapman and Hall, London UK, 6th ed., 1986.

[14] CRC Handbook of Chemistry and Physics, 76th ed. 1995–1996.

[15] Min-Yu Teng, Chi-Lan Li, Kueir-Rarn Lee and Juin-Yih Lai, Permselectivities of 3,3′,4,4′ benzydrol tetraacarboxylic dianhydrde based polyimide membranes for pervaporation, Desalination, 193 (2006) 144-151.

[16] Reverse Osmosis System Analysis, version 6.1, DOW, 16-2-2007.